International Journal of Nanomedicine

Dovepress
open access to scientific and medical research

Open Access Full Text Article

ORIGINAL RESEARCH

Polyvinylpyrrolidone-coated gold nanoparticles inhibit endothelial cell viability, proliferation, and ERK1/2 phosphorylation and reduce the magnitude of endothelial-independent dilator responses in isolated aortic vessels

This article was published in the following Dove Press journal:
International Journal of Nanomedicine

International Journal of Nanomedicine downloaded from https://www.dovepress.com/ by 149.170.165.59 on 29-Mar-2018
For personal use only.

Teba Mohamed[1,*]
Sabine Matou-Nasri[2,*]
Asima Farooq[3]
Debra Whitehead[3]
May Azzawi[1]

[1]School of Healthcare Science, Faculty of Science and Engineering, Manchester Metropolitan University, Manchester, UK; [2]Cell and Gene Therapy Group, Medical Genomics Research Department, King Abdullah International Medical Research Centre, National Guard Health Affairs, Riyadh, Saudi Arabia; [3]School of Science and the Environment, Faculty of Science and Engineering, Manchester Metropolitan University, Manchester, UK

*These authors contributed equally to this work

Correspondence: May Azzawi
School of Healthcare Science; Faculty of Science and Engineering, Manchester Metropolitan University, All Saints, Manchester M1 5GD, UK
Tel +44 161 247 3332; 3341
Email m.azzawi@mmu.ac.uk

Debra Whitehead
School of Science and the Environment, Faculty of Science and Engineering, Manchester Metropolitan University, All Saints, Manchester M1 5GD, UK
Tel +44 161 247 3332; 3341
Email d.whitehead@mmu.ac.uk

Background: Gold nanoparticles (AuNPs) demonstrate clinical potential for drug delivery and imaging diagnostics. As AuNPs aggregate in physiological fluids, polymer-surface modifications are utilized to allow their stabilization and enhance their retention time in blood. However, the impact of AuNPs on blood vessel function remains poorly understood. In the present study, we investigated the effects of AuNPs and their stabilizers on endothelial cell (EC) and vasodilator function.

Materials and methods: Citrate-stabilized AuNPs (12±3 nm) were synthesized and surface-modified using mercapto polyethylene glycol (mPEG) and polyvinylpyrrolidone (PVP) polymers. Their uptake by isolated ECs and whole vessels was visualized using transmission electron microscopy and quantified using inductively coupled plasma mass spectrometry. Their biological effects on EC proliferation, viability, apoptosis, and the ERK1/2-signaling pathway were determined using automated cell counting, flow cytometry, and Western blotting, respectively. Endothelial-dependent and independent vasodilator functions were assessed using isolated murine aortic vessel rings ex vivo.

Results: AuNPs were located in endothelial endosomes within 30 minutes' exposure, while their surface modification delayed this cellular uptake over time. After 24 hours' exposure, all AuNPs (including polymer-modified AuNPs) induced apoptosis and decreased cell viability/proliferation. These inhibitory effects were lost after 48 hours' exposure (except for the PVP-modified AuNPs). Furthermore, all AuNPs decreased acetylcholine (ACh)-induced phosphorylation of ERK1/2, a key signaling protein of cell function. mPEG-modified AuNPs had lower cytostatic effects than PVP-modified AuNPs. Citrate-stabilized AuNPs did not alter endothelial-dependent vasodilation induced by ACh, but attenuated endothelial-independent responses induced by sodium nitroprusside. PVP-modified AuNPs attenuated ACh-induced dilation, whereas mPEG-modified AuNPs did not, though this was dose-related.

Conclusion: We demonstrated that mPEG-modified AuNPs at a therapeutic dosage showed lower cytostatic effects and were less detrimental to vasodilator function than PVP-modified AuNPs, indicating greater potential as agents for diagnostic imaging and therapy.

Keywords: nanoparticles, gold, vascular, vasodilation, artery, cell culture

Plain-language summary

Gold nanoparticles have great clinical potential for drug delivery and imaging diagnostics. They are injected into the bloodstream to help diagnose and treat a number of conditions, including

© 2017 Mohamed et al. This work is published and licensed by Dove Medical Press Limited. The full terms of this license are available at https://www.dovepress.com/terms.php and incorporate the Creative Commons Attribution – Non Commercial (unported, v3.0) License (http://creativecommons.org/licenses/by-nc/3.0/). By accessing the work you hereby accept the Terms. Non-commercial uses of the work are permitted without any further permission from Dove Medical Press Limited, provided the work is properly attributed. For permission for commercial use of this work, please see paragraphs 4.2 and 5 of our Terms (https://www.dovepress.com/terms.php).

International Journal of Nanomedicine downloaded from https://www.dovepress.com/ by 149.170.165.59 on 29-Mar-2018
For personal use only.

cancer and vascular disease. Blood vessels are lined on the inside by cells that release mediators, which are essential for maintaining vessel health and in controlling vessel diameter to ensure that blood supply to tissues and organs matches demand. The nanoparticles were coated with polymer material to prevent their aggregation (clumping) and enhance their retention time in blood. The purpose of our work was to understand what effects gold nanoparticles and their coatings have on the function of blood vessels. We incubated isolated cells and vessels with coated gold nanoparticles and polymer coatings over short periods at the therapeutic dose currently used in animal/clinical studies. We demonstrate that gold nanoparticles are rapidly taken up by cells lining blood vessels. We also demonstrate that gold nanoparticles and their coatings affect the function of cells and dilation of blood vessels. Our study will help guide clinicians on the use of gold nanoparticles and type of coatings that has least damaging effects on blood vessels.

Introduction

Gold nanoparticles (AuNPs) present a growing potential modality in biomedical research and clinical applications. As carriers of small biological compounds (eg, RNA, proteins, drugs), AuNPs can be engineered to enable targeting for the treatment of such conditions as diabetes, cancer, and vascular diseases through drug delivery and in diagnostic imaging as contrast agents.[1,2] For example, AuNPs have been utilized in clinical trials for the treatment of lung and more recently prostate cancer. These comprise a 1–3 nm gold core with a 100–120 nm silica shell, designed for precise thermal ablation of tumors following stimulation with a near-infrared energy source.[1,3] Due to the high tendency of AuNPs to aggregate in solution,[4] they are citrate-stabilized and often surface-modified using organic polymer coatings. These polymers are hydrophilic chain-structured macromolecules that allow the AuNPs to remain well dispersed even at high salt concentrations. The polymers cause steric repulsion and prevent aggregation of the colloid particles, making them good stabilisers.[5] These include thiolated mercapto polyethylene glycol (mPEG) and polyvinylpyrrolidone (PVP). Aurimune (CYT6091) is a novel AuNP currently planned for Phase II clinical trials for the treatment of late-stage cancer.[6] Colloidal AuNPs (27 nm) have been surface-modified with PEG and tagged with TNFα to enable targeted delivery to tumors.[7] As potential drug-delivery and imaging modalities, AuNPs are hence injected intravenously into the bloodstream.[1] As such, endothelial cells (ECs) lining blood vessels constitute the first site of exposure to these NPs. ECs play central roles in hemostasis and the modulation of blood vessel function through the release of mediators, in particular vasodilators, such as nitric oxide (NO), which has key antithrombogenic properties to help maintain vascular health.

Although AuNPs have been documented as biocompatible and nontoxic for cells,[8,9] evidence suggests that they can affect EC viability and function,[10] inducing apoptosis, upregulation of inflammatory mediators,[11] and affecting signal-transduction pathways, including reduced phosphorylation of ERK1/2, and Akt/PKB, which are necessary for cell function.[12,13] Furthermore, AuNPs can induce oxidative stress and generate reactive oxygen species, which can quench NO, thus affecting vascular function.[14,15] The cytotoxic effects of AuNPs have been shown to be dependent on cell type, NP size, shape, dosage, and in particular, surface chemistry.[15,16] The importance of AuNP-surface modification has thus been highlighted, eg, PEG surface modification of 50 nm-length gold nanorods has been shown to reduce EC death in comparison to polyelectrolyte capping.[17] In addition, PVP is widely accepted as a biocompatible polymer material.[18] For example, in vitro culture studies examining the influence of PVP coating on the immunotoxicity of graphene oxide have suggested that T-lymphocyte apoptosis is significantly delayed and less immunogenic than pure graphene oxide.[19] However, the impact of AuNP stabilizers on the viability of ECs and the function of healthy blood vessels remains poorly investigated. The aim of the present study was to determine the influence of AuNPs and their stabilizers on EC and vasodilator function of isolated aortic murine vessels ex vivo, in order to inform their safe clinical use.

Materials and methods

Reagents and drugs

All reagents were obtained from Sigma-Aldrich (St Louis, MO, USA), unless otherwise stated. Physiological salt solution (PSS) was prepared using the following chemical composition (mM): 119 NaCl, 4.7 KCl, 1.2 $MgSO_4 \cdot 7\ H_2O$, 25 $NaHCO_3$, 1.17 KH_2PO_4, 0.03 $K_2EDTA \cdot 2H_2O$, 5.5 glucose, and 1.6 $CaCl_2 \cdot 2H_2O$, pH 7.4. Potassium PSS (KPSS; 60 mM) was prepared using the following chemical composition (mM): 78.2 NaCl, 60 KCl, 1.2 $MgSO_4 \cdot 7\ H_2O$, 25 $NaHCO_3$, 1.17 KH_2PO_4, 0.03 $K_2EDTA \cdot 2H_2O$, 5.5 glucose and 1.6 $CaCl_2 \cdot 2H_2O$, pH 7.4, as previously described.[20]

Synthesis and characterization of PVP and mPEG-modified gold NPs

Monodispersed AuNPs (12±3 nm) were synthesized according to Turkevich et al's method (using chloroauric acid Au^{3+} reduced by sodium citrate)[21] and characterized by transmission electron microscopy (TEM). PVP-modified AuNPs were prepared by dissolving 0.0036 g of PVP (molecular weight 8,000 Da) in 1 mL deionized H_2O, and 500 µL stock was left to stir with the gold seeds for 24 hours. The mPEG-modified

International Journal of Nanomedicine downloaded from https://www.dovepress.com/ by 149.170.165.59 on 29-Mar-2018
For personal use only.

AuNPs were prepared by adding 0.125 mL (from a stock of 1.44×10^{-5} g/mL of mPEG molecular weight 5,000 Da) to 0.5 mL AuNPs and left to stir for 24 hours. To check the stability of the synthesized AuNPs after dispersion in PSS, water, or complete medium, samples were characterized by assessing their ultraviolet (UV)-visible spectra using a spectrophotometry. Fourier-transform infrared spectroscopy (FTIR)/diffuse reflectance infrared FT spectroscopy (DRIFTS) were performed to determine the fingerprints of the polymer-modified AuNPs and their stabilizers. A background spectrum was initially run using Omnic software (Thermo Fisher Scientific) before samples were analyzed. Additionally, the functional groups attached on the polymer-modified AuNPs were analyzed by surface-enhanced Raman scattering.

Cell-culture studies

Bovine aortic ECs (BAECs) were previously isolated and cultured as described by Sattar et al,[22] in accordance with Manchester Metropolitan University's institutional review board guidelines and ethics committee approval (FAETC/09-10/19). Cells were cultured in complete medium composed of DMEM (Thermo Fisher Scientific) supplemented with 15% heat-inactivated FBS (ICN Biochemicals, Basingstoke, UK), 2 mM glutamine, and antibiotics (100 µg/mL streptomycin and 100 IU/mL penicillin) into a 75 cm^2 flask precoated with 0.1% gelatin. BAECs were incubated at 37°C in 5% CO_2 and 95% saturated atmospheric humidity. Every 2–3 days, cells were passaged following enzymatic digestion with 0.05% trypsin–0.02% EDTA and split at a ratio of 1:2 or 1:3. At confluence, BAECs were characterized by their typical cobblestone morphology. The cells were used throughout the study between passages 4 and 9. Cells were exposed to AuNPs at 2.9 µg/mL.

To assess EC proliferation, viability, and apoptosis, BAECs (4×10^4 cells/well) were seeded in complete medium in a 24-well plate. After 4 hours' incubation, the medium was replaced with serum-poor medium (SPM; medium supplemented with 2.5% FBS to reduce adsorption of unknown serum proteins on AuNP surface) with or without AuNPs, and concentration determined by preliminary studies. After 24 and 48 hours of incubation, cells were detached using 0.05% trypsin–0.02% EDTA and counted using a Beckman Coulter counter (Brea, CA, USA). Each condition was performed in triplicate and each experiment repeated three times.

Flow-cytometry analysis was used to assess cell viability based on the exclusion of the nonvital membrane impermeant DNA dye propidium iodide (PI) conjugated to phycoerythrin (PE) staining using the FL3 channel on a FACScan instrument. Viable cells corresponding to the PI-unstained cell samples prior to analysis were then set on stop count and examined on a forward scatter versus FL3 (PI) dot-plot staining. Normalization of the data was done using fluorescence-activated cell-sorting (FACS) software and related to the unstained cells.

For the study of apoptosis and necrosis, cells were treated with 1 µg/mL staurosporine, a potent proapoptotic protein-kinase inhibitor. The positive control (staurosporine-treated cells) was used to determine whether cells underwent apoptosis after exposure to modified and unmodified AuNPs along with their stabilizers after 2 and 24 hours of incubation. Cells were stained as described in an annexin V–fluorescein isothiocyanate (FITC) apoptosis-detection kit containing PI-PE. Apoptotic cells were characterized by the binding of annexin V to phosphatidylserine residues exposed to the outer membrane due to the loss of membrane integrity, also defined as annexin V^+/PI^- cells. Necrotic cells were characterized by annexin V in conjunction with the binding of PI as an indicator of the loss of plasma and nuclear membrane integrity, also defined as annexin V^+/PI^+ (late apoptotic/necrotic cells) and annexin V^-/PI^+ (necrotic cells). The percentage of apoptotic or necrotic cells was obtained using the flow-cytometry analysis software. Each experiment was repeated at least three times. The fate of internalized AuNPs in BAECs was determined by TEM. After AuNP incubation, cells were fixed with 2% paraformaldehyde and processed. Ultrathin 70 nm sections were cut, placed on copper grids and observed using TEM (Tecnai 12 BioTwin at 80 kV).

For Western blot analysis, BAECs (6×10^5 cells/well) were seeded in complete medium in a six-well plate. After 48 hours of incubation, the medium was renewed with SPM for a further 24 hours' incubation, then AuNPs, AuPVP, PVP (5.9×10^{-7} µM), AumPEG, or mPEG (9.25×10^{-9}) were added for 10 minutes' exposure. Cell-lysate preparation, protein separation (by 12% sodium dodecyl sulfate-polyacrylamide gel electrophoresis), and transfer of separated proteins onto nitrocellulose membranes were performed as previously described.[23] Nitrocellulose membranes were then stained with the following primary antibodies, overnight on a rotating shaker: mouse monoclonal antibodies to phospho-ERK1/2 (p-ERK1/2, Tyr204 of ERK1, 1:1,000 dilution) and rabbit polyclonal antibodies to total ERK1/2 (C-16) (t-ERK1/2; 1:1,000 dilution), provided by Santa Cruz Biotechnology. After being washed five times for 10 minutes in TBS–Tween at room temperature, filters were stained with either rabbit antimouse or goat antirabbit HRP-conjugated secondary antibodies diluted in TBS–Tween containing 5% defatted milk (1:1,000 dilution) for 1 hour at room temperature with

International Journal of Nanomedicine downloaded from https://www.dovepress.com/ by 149.170.165.59 on 29-Mar-2018
For personal use only.

continuous shaking. After a further five washes in TBS–Tween, proteins were visualized using electrochemiluminescence detection (GE Healthcare UK, Little Chalfont, UK) and analyzed using GeneSnap software with the GeneTools image analyzer (Syngene, Cambridge, UK).

Vascular function studies

Segments of aortae (from male Wistar rats) were freshly isolated and surrounding perivascular fat carefully removed under a dissecting microscope (following institutional approval FAETC/09-10/19) in accordance with guidelines issued by the European Commission (directive 86/609/EEC). Aortic rings (2–3 mm in length) were cut, then suspended between two fine steel wires and placed in an oxygenated organ bath containing PSS. The rings were then loaded passively to 2 *g* tension to stabilize over 1 hour using a Harvard isometric transducer. Vessels were preconstricted with KPSS and dilated using the endothelium-dependent agonist acetylcholine (ACh; 0.01–100 μM) before and after incubation with AuNPs (2.9 μg/mL) for 30 minutes. The influence of polymers alone (10 nM–0.1 μM) on dilator function was also examined.

The presence of modified and unmodified AuNPs within the aortic vessels after 30 minutes' incubation was determined using inductively coupled plasma mass spectrometry (ICP-MS; PerkinElmer, Waltham, MA, USA). Briefly, the vessel was firstly weighed before incubation with the experimental conditions (AuNPs, AumPEG, or AuPVP). Vessel weight was recorded and lysate buffer (0.5 mL containing 0.5 g sodium dodecyl sulfate, 0.2925 g NaCl, 0.394 g tris, 0.03 g tris[hydroxylmethyl]aminomethane) was added for 48 hours at room temperature. Each tube was mixed with 1 mL high-purity (70%) nitric acid to dissolve the vessel. Glass tubes were placed in an oil bath at 200°C for 3 hours and analyzed.

Statistical analysis

For vascular function studies, results are expressed as mean ± SEM, and one-way analysis of variance with Bonferroni correction test was used for comparison of two groups. For cellular studies, an unpaired Student's *t*-test was used for comparison of two groups, and results are expressed as means ± SD. For each test applied, a value of $P<0.05$ was considered significant.

Results

Characterization of gold NPs

TEM of unmodified AuNPs showed they were monodispersed (12±3 nm in diameter) and spherical (Figure 1A). The addition of organic polymer-composite coatings (PVP and mPEG) did not affect the overall size or sphericity of AuNPs. With UV-visible spectroscopy, it was possible to identify the characteristic plasmon resonance peak at 525 nm wavelength. As the surface-plasmon position is very sensitive to surface interactions, any NP aggregation can result in loss of the plasmon peak, and hence aggregation was assessed using plasmon absorption. UV-visible spectra confirmed that the unmodified AuNPs were stable in the presence of ultrapure water. The characteristic plasmon resonance peak was identified at 525 nm wavelength; however, when dispersed in PSS the peak was lost, indicating particle aggregation. The plasmon resonance peak was also evident when the PVP- and mPEG-modified AuNPs were suspended in both water and PSS, demonstrating that AuNPs were stable after surface modification using polymers (Figure 1B). Furthermore, both modified and unmodified AuNPs were stable in DMEM cell-culture media; however, the slight shift in the plasmon peak indicated that there was a change in the NP-surface environment (due to the presence of proteins that are likely to have adsorbed on to the AuNP surface [Figure 1C]).

FTIR-DRIFTS spectra of PVP- and mPEG-modified AuNPs were compared with spectra from PVP and mPEG alone. PVP peaks at 1,660 cm^{-1} and 1,200 cm^{-1} corresponded to the C=O and C–N vibrations in PVP. Absorption peaks at 1,650 cm^{-1} and 1,641 cm^{-1} are characteristics of pyrrolidinyl groups in PVP.[24] These were also observed on the PVP-modified AuNPs, confirming surface functionalization. Evidence for mPEG functionalization of the AuNPs was demonstrated by characteristic absorption in mPEG at 1,103 cm^{-1}, corresponding to C–O–C vibration, and the peak at 1,641 cm^{-1} corresponds to the C=O from the residual citrate groups still present.[25] The C=O vibration at 1,637 cm^{-1} identified upon analysis of the citrate-stabilized AuNPs relates to the presence of sodium citrate[26] (Figure 2). The functional groups on our AuNPs were also confirmed using surface-enhanced Raman spectroscopy analysis (Figure S1).

Effect of gold NPs on isolated endothelial cells in vitro

TEM clearly demonstrated the uptake of both unmodified and modified AuNPs by cultured BAECs at different incubation times (Figure 3). After 2 hours of cell exposure, there was an increase in AuNP uptake (32±5 AuNPs) compared to the low number observed after 30 minutes' exposure (5±0 AuNPs). Interestingly, there was a greater number of AuNPs and AuPVP internalized by the cells after 24 hours (638±156 and 233±92, respectively). However, after 48 hours of cell exposure, there was a higher uptake of AuPVP (700±92),

International Journal of Nanomedicine downloaded from https://www.dovepress.com/ by 149.170.165.59 on 29-Mar-2018
For personal use only.

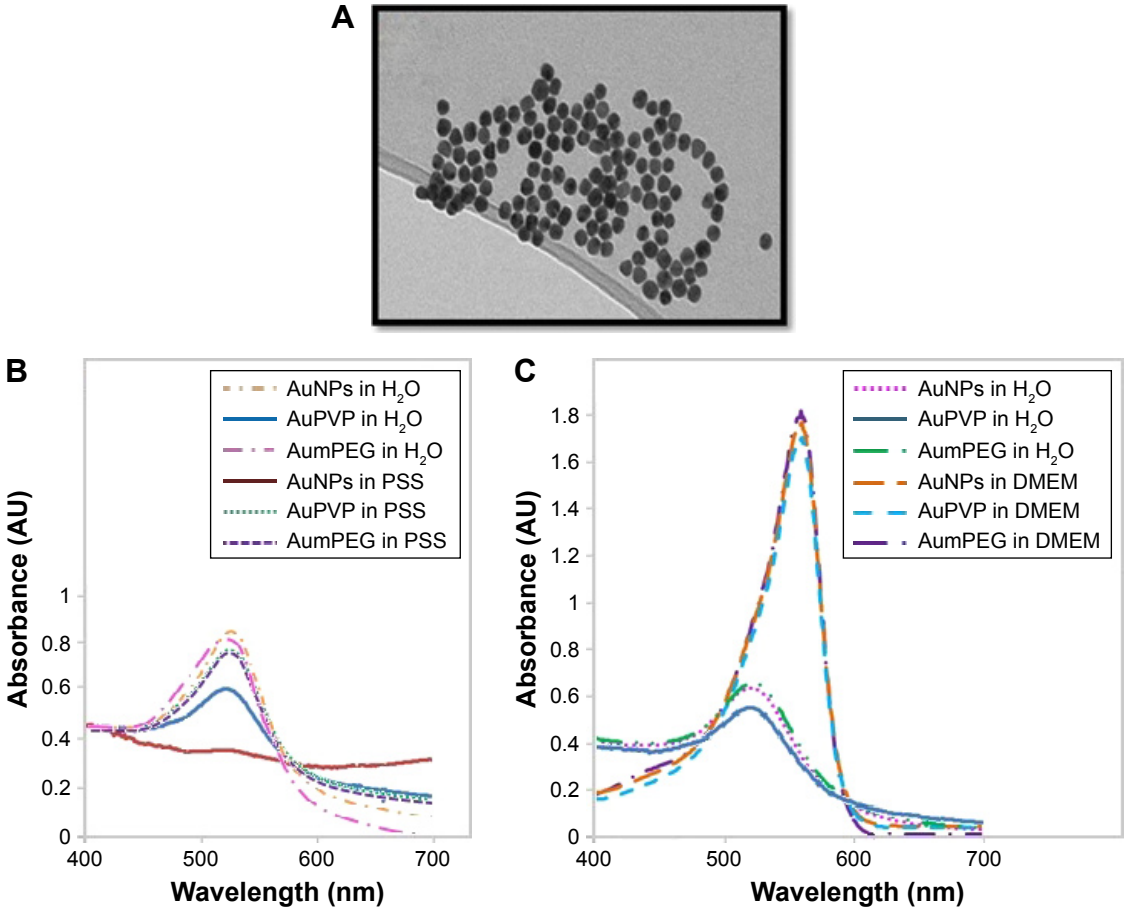

Figure 1 Gold nanoparticle (AuNP) synthesis and characterization.
Notes: (**A**) Transmission electron micrography of spherical monodispersed citrate-stabilized AuNPs (12±3 nm); (**B**, **C**) Ultraviolet-visible absorbance spectra of AuNP stability after modification with PVP and mPEG in physiological salt solution (PSS) and culture media.
Abbreviations: PVP, polyvinylpyrrolidone; mPEG, mercapto polyethylene glycol.

but significantly less uptake of AumPEG (16±4). Both modified and unmodified AuNPs were observed to be localized in endosomes within the cytoplasm (Figure 3). AuNP uptake had no influence on the standard polygonal shape of the cells.

In the absence of AuNPs, there was no significant change in cell proliferation after 48 hours' exposure compared with the control (untreated cells) obtained after 24 hours' exposure. The addition of unmodified AuNPs significantly decreased cell proliferation after 24 and 48 hours ($P<0.001$ and $P=0.01$, respectively). When the BAECs were exposed to PVP-modified AuNPs, significant inhibition (30%, $P<0.01$) was observed after 24 hours (Figure 4). Similarly, there was significant inhibition in cell proliferation when BAECs were exposed to the composite polymers PVP (2.04×10^{-7} g/mL, $P<0.01$), PEG (4 µg/mL, $P=0.01$), mPEG (7.4×10^{-8} g/mL, $P<0.001$), and modified AuNPs, including AuPVP and AumPEG ($P<0.001$), after 24 hours. In contrast to AuNPs, the inhibitory effects of modified AuNPs on cell proliferation were reduced after 48 hours' exposure when compared with the control.

We determined the viability of BAECs using FACS following exposure to modified and unmodified AuNPs and their stabilizers after 30 minutes and 2, 24, and 48 hours. In the absence of AuNPs, short (30 minutes and 2 hours) and long (24 and 48 hours) exposure did not affect the high cell viability (around 95%) compared with the control (untreated cells at 30 minutes). The addition of unmodified and modified AuNPs to SPM slightly decreased cell viability by 5% after 30 minutes' exposure, with a further decrease by 5% after 2 hours' exposure followed by 20% reduction in cell viability, compared with the respective control (untreated cells after 30 minutes and 2 and 24 hours) (Figure 5). After 48 hours' exposure, unmodified and mPEG-modified AuNPs lost their inhibitory effect on cell viability observed after 24 hours' exposure, which displayed high cell viability compared with untreated cells (Figures 5 and S2).

The apoptotic and necrotic status of BAECs were determined by flow-cytometry analysis through the double staining of annexin V–FITC and nonvital dye PI-PE. Untreated cells were defined as a negative control and staurosporine,

International Journal of Nanomedicine downloaded from https://www.dovepress.com/ by 149.170.165.59 on 29-Mar-2018
For personal use only.

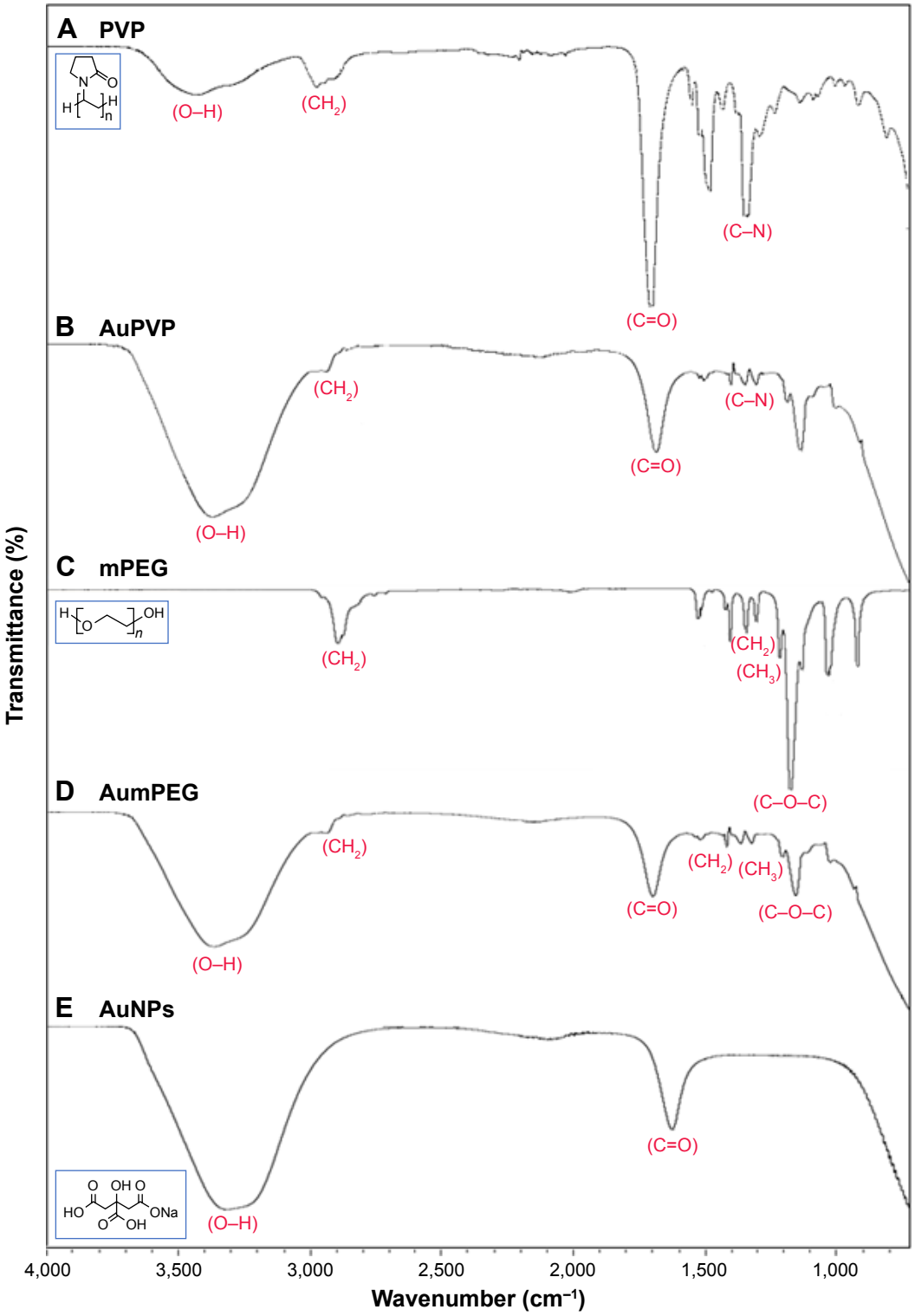

Figure 2 FTIR spectra for stabilizers and unmodified and modified AuNPs.
Note: (**A**) PVP, (**B**) AuPVP, (**C**) mPEG, (**D**) AumPEG, and (**E**) AuNPs, illustrating characteristic absorption peaks.
Abbreviations: FTIR, Fourier-transform infrared spectroscopy; AuNPs, gold nanoparticles; PVP, polyvinylpyrrolidone; mPEG, mercapto polyethylene glycol.

a protein-kinase inhibitor, used as a positive control for induction of apoptosis. After 2 hours' exposure, the cell population treated with modified and unmodified AuNPs displayed about 30%–40% apoptotic cells compared to 1%–3% within untreated cells (Figure 6). A decrease in the percentage of apoptotic cells was observed after 24 hours of cell exposure to AuNPs, while the percentage of apoptotic cells was increased slightly in the presence of either polymer composites or modified

International Journal of Nanomedicine downloaded from https://www.dovepress.com/ by 149.170.165.59 on 29-Mar-2018
For personal use only.

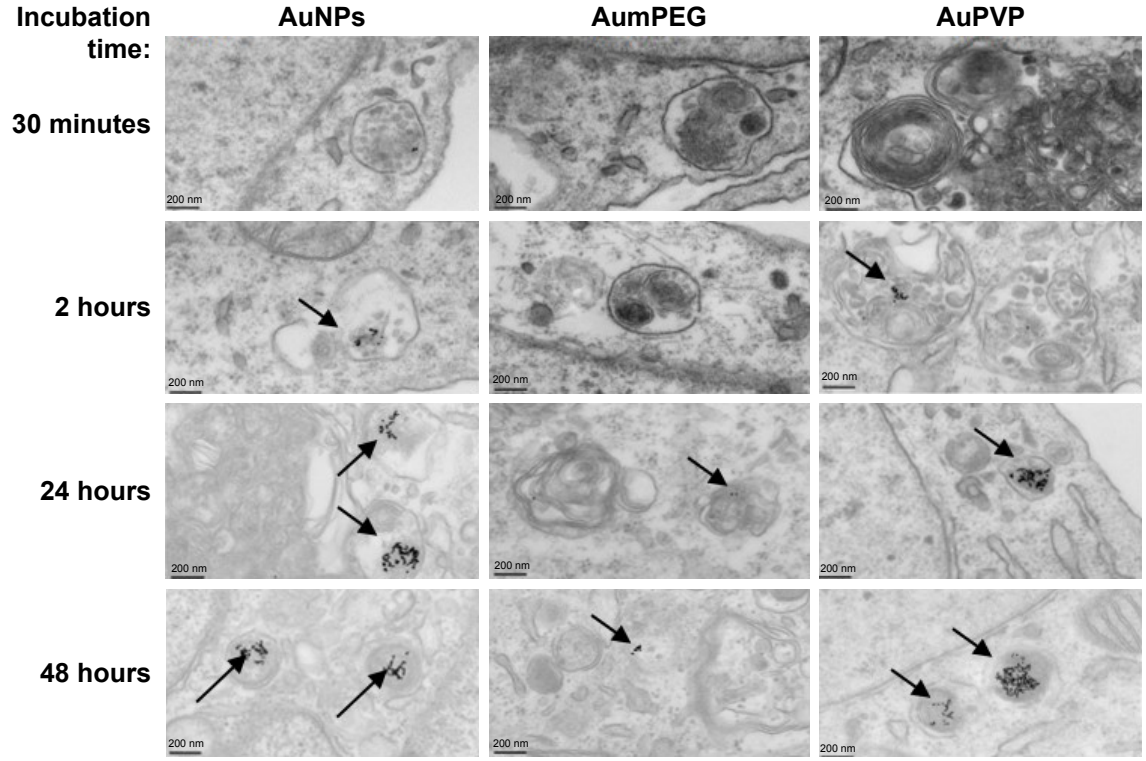

Figure 3 Gold nanoparticle (AuNP) uptake by BAECs in culture.
Notes: Transmission electron micrographs showing the time course of AuNP uptake (citrate-stabilized and mPEG- and PVP-modified) by BAECs. AuNPs are identified as spherical structures inside endosomes within the endothelial cells (arrows).
Abbreviations: BAECs, bovine aortic endothelial cells; mPEG, mercapto polyethylene glycol; PVP, polyvinylpyrrolidone.

AuNPs (Figure 6). No necrotic cells were detected after 2 hours' incubation with polymer composites or unmodified/modified AuNPs, but 45% necrotic cells were determined when exposed to PVP compared with the control (untreated cells) (Figure 6). This PVP necrotic effect mostly disappeared with exposure time, as a weak necrotic effect was detected compared with the control (untreated cells) (Figure 6). In contrast to PVP necrotic effect, after 24 hours' exposure, the cell population treated with mPEG displayed about 30% necrotic cells compared to 18% within untreated cells (control) (Figures 6 and S2).

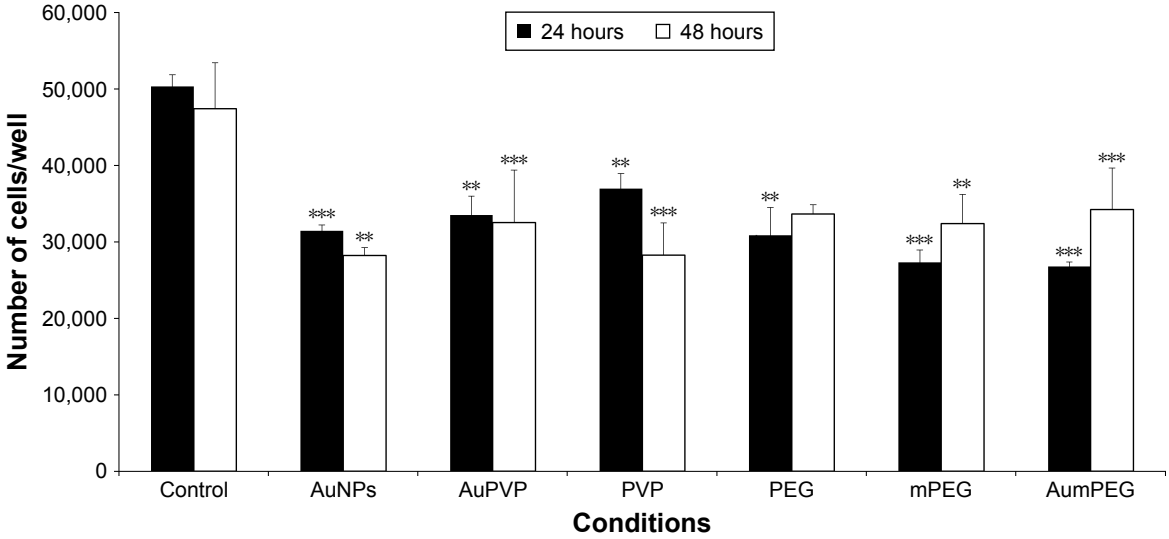

Figure 4 Inhibitory effects of stabilizers and unmodified and modified AuNPs on BAEC proliferation.
Notes: $^{**}P<0.01$; $^{***}P<0.001$. Results presented as mean ± SD. Three independent experiments.
Abbreviations: AuNPs, gold nanoparticles; BAEC, bovine aortic endothelial cell; mPEG, mercapto polyethylene glycol; PVP, polyvinylpyrrolidone.

International Journal of Nanomedicine downloaded from https://www.dovepress.com/ by 149.170.165.59 on 29-Mar-2018
For personal use only.

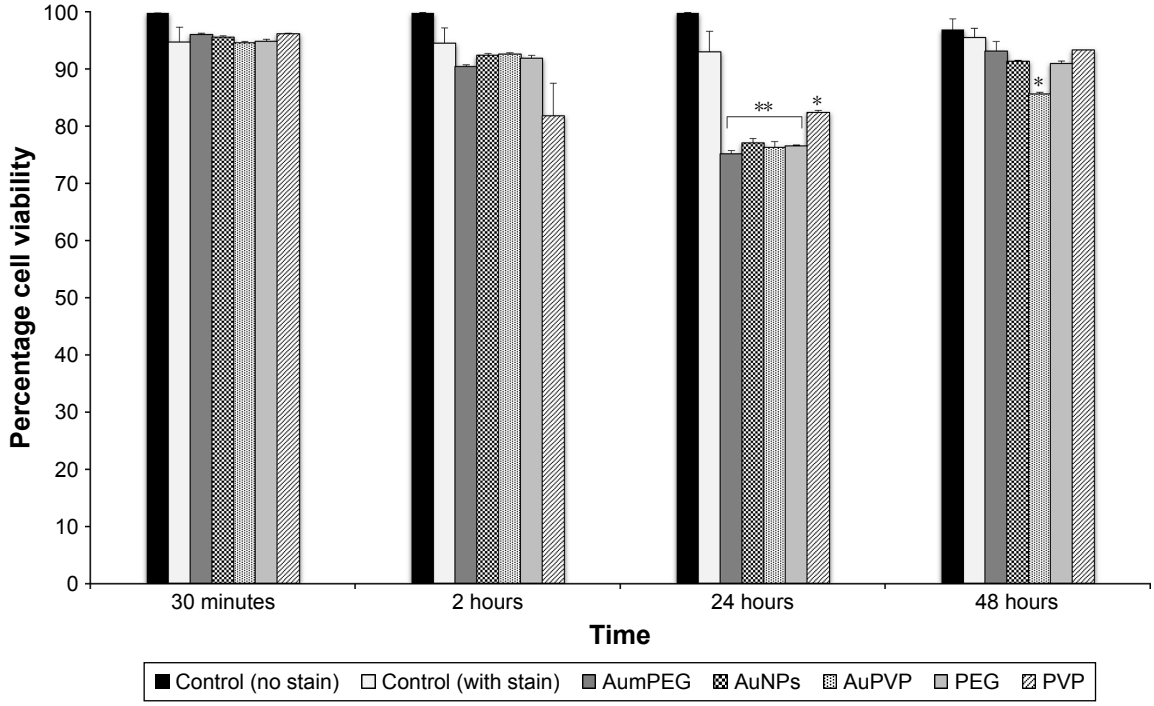

Figure 5 The influence of stabilizers and unmodified and modified AuNPs on BAEC viability using flow cytometry.
Notes: *$P<0.05$; **$P<0.01$. Percentage cell viability of BAECs in the untreated cells and cells treated with stabilizer (PVP), non-modified and modified AuNPs (AuPVP, AumPEG) after 30-minute and 2–24- and 48-hour exposure based on three independent experiments. Results presented as mean ± SD.
Abbreviations: AuNPs, gold nanoparticles; BAEC, bovine aortic endothelial cell; PVP, polyvinylpyrrolidone; mPEG, mercapto polyethylene glycol.

To check the functional integrity of the endothelium, cultured BAECs were exposed to various concentrations of the endothelium-dependent vasodilator ACh (1, 10, and 100 µM) for 10 minutes. Mediated through muscarinic receptors, ACh has been demonstrated to induce several signaling pathways, including the survival pathway involving ERK1/2. The effect of ACh concentrations on ERK1/2 phosphorylation was assessed by Western blot analysis. When compared to untreated cells (control), ACh concentrations induced phospho-ERK1/2 expression at all concentrations used, with a peak of stimulation attained in the presence of 10 µM ACh (fivefold increase) (Figure 7A). As NPs have been suggested to influence the phosphorylation or dephosphorylation of regulatory proteins involved in vascular function,

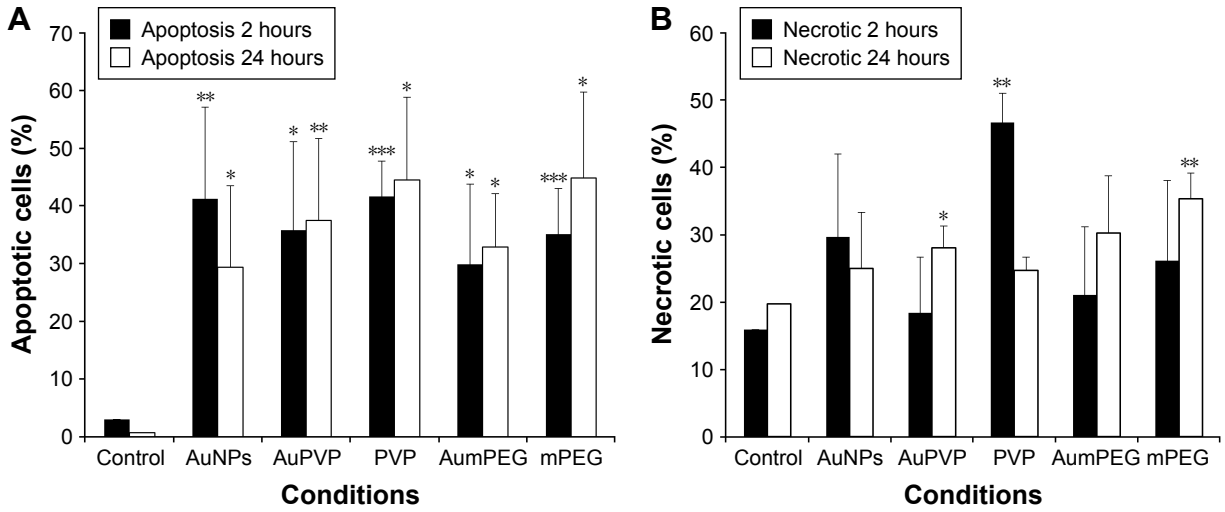

Figure 6 Induction of apoptosis and necrosis by stabilizers and unmodified and modified AuNPs in BAECs.
Notes: *$P<0.05$; **$P<0.01$; ***$P<0.001$. Apoptosis (**A**) and necrosis (**B**) of BAECs in untreated cells and cells treated with stabilizer (PVP) and unmodified and modified AuNPs (AuPVP, AumPEG) after 2- and 24-hour exposure based on three independent experiments. Results presented as mean ± SD.
Abbreviations: AuNPs, gold nanoparticles; BAECs, bovine aortic endothelial cells; PVP, polyvinylpyrrolidone; mPEG, mercapto polyethylene glycol.

International Journal of Nanomedicine downloaded from https://www.dovepress.com/ by 149.170.165.59 on 29-Mar-2018
For personal use only.

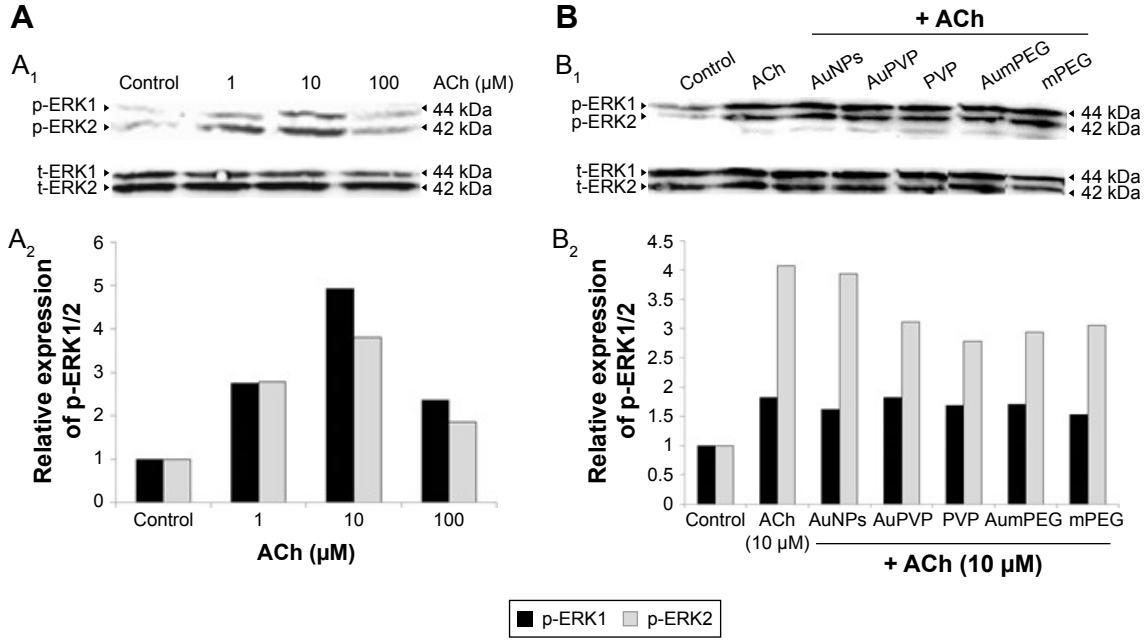

Figure 7 Modulatory effects of stabilizer and unmodified and modified AuNPs on ACh-induced ERK1/2 phosphorylation in BAECs.

Notes: (**A**) Representative Western blot analysis (A_1) showing the stimulatory effect of 1/10/100 μM ACh on ERK1/2 phosphorylation (p-ERK1/2) in BAECs after 10 minutes' exposure compared to untreated cells (control); relative expression of p-ERK1/2 calculated as a ratio to ERK1/2 expression, the loading control (A_2). (**B**) Representative Western blot analysis (B_1) showing the modulatory effects of 10 μM ACh-induced ERK1/2 phosphorylation in the absence or in the presence of stabilizer (PVP) and non-modified and unmodified AuNPs (AuPVP, AumPEG) in BAECs after 10 minutes' incubation compared to untreated cells (control). The bar graph shows the relative expression of p-ERK1/2 calculated as a ratio to ERK1/2 expression, the loading control (B_2).

Abbreviations: AuNPs, gold nanoparticles; ACh, acetylcholine; BAECs, bovine aortic endothelial cells; PVP, polyvinylpyrrolidone; mPEG, mercapto polyethylene glycol; t-ERK, total ERK.

we investigated the potential modulatory effects of polymer-modified AuNPs on ACh-stimulated ECs. BAECs were thus exposed to 10 μM ACh in the presence of modified and unmodified AuNPs to assess ERK1/2 phosphorylation subsequently. Both unmodified and modified AuNPs, as well as polymers alone or combined with ACh, caused a reduction in ERK2 phosphorylation when compared to ACh-induced phospho-ERK2 expression (Figure 7B). A significant reduction in expression was observed after AuPVP, PVP, and AumPEG incubation ($P<0.05$).

Effect of gold NPs on vascular function

TEM indicated that the unmodified AuNPs had aggregated and were located within the lumen of the vessel. They were seen close to the surface of ECs. There was no evidence that AuNPs had entered the cell. On the other hand, PVP-modified NPs were identified within ECs. They were located within endosomal structures, but not freely within the cytoplasm, suggesting that uptake was by the process of endocytosis. Very few mPEG-modified AuNPs were identified in ECs when added at 2.9 μg/mL. However, once the NP concentration was increased, greater uptake was detected (Figure 8). ICP-MS analysis indicated a high degree of uptake of unmodified AuNPs (0.45 ppm, 13.95%) compared to PVP (0.14 ppm, 4.4%) and mPEG-modified NPs at 2.9 μg/mL. At 5.8 μg/mL, both uptake of PVP- (0.38 ppm, 6.46%) and mPEG- (0.35 ppm, 6.07%)-modified AuNPs increased, but was nonetheless still lower than that of the unmodified AuNPs (highest uptake at 0.74 ppm, 23.95%) (Figure 8).

All vessels constricted to high-potassium PSS (60 mM, KPSS). There was no significant difference in the degree of constriction after vessels were incubated in unmodified AuNPs (2.31±0.28 g/tension, n=5), PVP-modified AuNPs (2.31±0.35 g/tension, n=5), mPEG-modified AuNPs (2.26±0.18 g/tension, n=5), PVP alone (2.312±0.139 g/tension, n=5), PEG alone (2.71±0.13 g/tension, n=5), or mPEG alone (2.57±0.18 g/tension, n=5) compared to PSS (2.00±0.124 g/tension, n=5).

ACh and sodium nitroprusside (SNP) induced a concentration-dependent dilator response in all preconstricted vessels. Incubation with citrate-stabilized AuNPs had no overall effect on ACh-induced endothelial-dependent dilator responses (n=5), but significantly reduced SNP-induced dilator responses (Figure 9). PVP-modified AuNPs had no overall influence on endothelial-dependent dilator responses. However, PVP alone (at 5.9×10^{-7} μM, identified as the minimum concentration required to prevent aggregation) caused a significant reduction in ACh dilator responses at 10–100 μM (ACh) ($P<0.05$) when compared to PSS. Vessel incubation in AuPVP affected SNP dilator responses;

International Journal of Nanomedicine downloaded from https://www.dovepress.com/ by 149.170.165.59 on 29-Mar-2018
For personal use only.

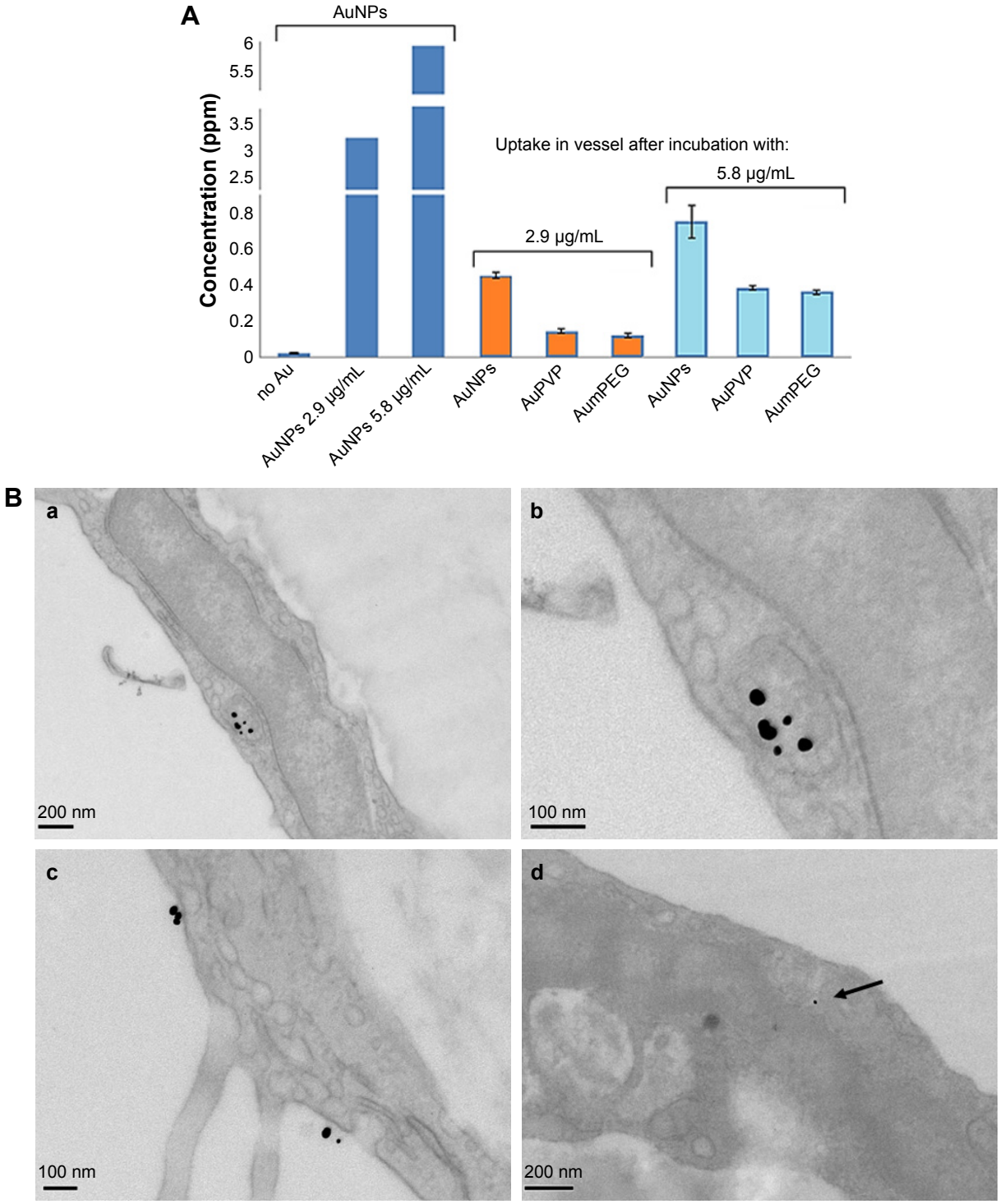

Figure 8 Gold nanoparticle (AuNP) uptake by aortic vessels.
Notes: (**A**) Determination of AuNP uptake using inductively coupled plasma analysis. Concentration of unmodified and polymer-modified AuNPs within aortic vessels after 30 minutes' exposure. Error bars are SEM. (**B**) Representative transmission electron micrography illustrating the uptake of PVP-modified AuNPs into endosomal structures (a; b at higher magnification), and also on the surface of endothelial cells lining the aortic vessel (c), within 30 minutes' exposure. Very few mPEG-modified AuNPs are seen as spherical dense structures within the endothelial cells (d, arrow) when exposed to the higher concentration.
Abbreviations: PVP, polyvinylpyrrolidone; mPEG, mercapto polyethylene glycol.

a significant reduction in dilator response was obtained at 0.001–0.01 µM (SNP, $P<0.001$), with a further reduction at 0.1 µM ($P<0.01$). PVP alone led to a small reduction in SNP responses (Figure 9). There was no significant attenuation in ACh responses after incubation with mPEG-modified AuNPs. Incubation in PEG alone had no overall effect on ACh dilator responses. mPEG-modified AuNPs at 2.9 µg/mL had no overall effect on SNP dilator responses (Figure 9). At a

International Journal of Nanomedicine downloaded from https://www.dovepress.com/ by 149.170.165.59 on 29-Mar-2018
For personal use only.

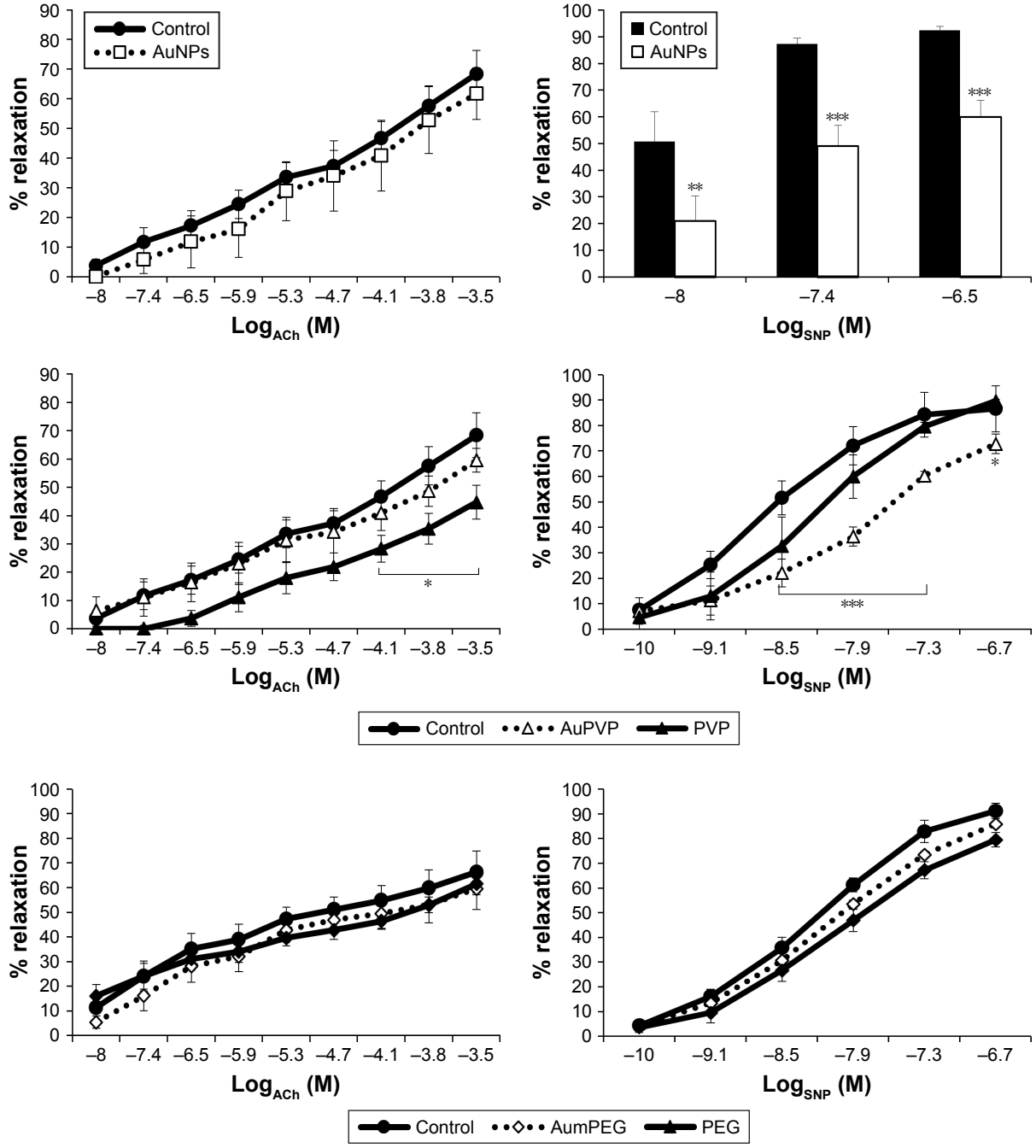

Figure 9 Influence of stabilizers and unmodified and modified AuNPs on dilator responses of aortic vessels.
Notes: *$P<0.05$; **$P<0.01$; ***$P<0.001$. Endothelial-dependent (ACh) and independent (SNP) dilator responses of preconstricted aortic vessels after 30 minutes' exposure ex vivo. Error bars are SEM.
Abbreviations: AuNPs, gold nanoparticles; ACh, acetylcholine; SNP, sodium nitroprusside; PVP, polyvinylpyrrolidone; mPEG, mercapto polyethylene glycol.

higher concentration of 5.8 µg/mL, mPEG-modified AuNPs led to a significant reduction in dilator responses compared to PSS control at most ACh concentrations (Figure S3).

Discussion and conclusion

AuNP fabrication and surface modification remain a critical step to avoid aggregation and increase efficiency of drug release. In the present study, we demonstrated that surface modification of AuNPs reduced their uptake by ECs compared to unmodified AuNPs within 30 minutes of exposure. We showed that mPEG-modified AuNPs had less inhibitory effects on EC proliferation, viability, and ACh-induced cell and vascular functions than PVP-modified AuNPs.

A slight change in the ionic strength of the microenvironment, such as that observed in many bodily fluids (including blood plasma), is known to be the cause of AuNP aggregation,

International Journal of Nanomedicine downloaded from https://www.dovepress.com/ by 149.170.165.59 on 29-Mar-2018
For personal use only.

which leads to a shift in the surface-plasmon resonance peak. AuNP-surface modification using PVP and mPEG enables stearic stabilisation[27,28] and significantly increases the stability of NPs in NaCl.[29] Indeed, nanomaterials that are completely coated in PVP have been shown not to aggregate even at high salt concentration.[30] PVP has been demonstrated to stabilize AuNPs by the interaction of the lone pair of electrons from nitrogen and oxygen atoms in its polar groups with the AuNP surface.[31] In our present study, AuNP aggregation in PSS was the result of complex formation of citrate anions with Na^+ cations in the PSS. The stability of unmodified AuNPs in cell-culture medium may be due to the presence of FBS and cellular proteins that absorb on the surface of AuNPs.[27] These provide stability to the AuNPs, as demonstrated by our UV-visible spectra, which did not show any loss of surface-plasmon resonance (at 525 nm) after exposure to the cell-culture medium.[32] Evidence for PVP and mPEG functionalization on AuNPs was confirmed using FTIR, as has been previously demonstrated.[26] Surface-enhanced Raman scattering analysis also confirmed the presence of functional groups on surface-modified AuNPs.

In the present study, AuNPs were internalized within endosomal structures inside the cytoplasm of BAECs. We show that cellular uptake of AuNPs was dependent on incubation time and type of stabilizers used.[27] This is in agreement with previous research that has also demonstrated that AuNP uptake is dependent on surface chemistry, size, shape, and dosage.[27] Freese et al elegantly demonstrated the size- and coating-dependent uptake of AuNPs within ECs.[33] While intracellular uptake of AuNPs has been shown to enhance the effects of radiation doses,[34] the dynamics of uptake can vary depending on cell type and the physical dimensions of the AuNPs.[35] By examining the kinetics of the uptake of 14–100 nm spherical and rod-shaped AuNPs into HeLa cells, maximum uptake has been demonstrated for 50 nm AuNPs with a half-life of 1.9 hours.[35] AuNP uptake by our ECs was evident within 30 minutes' incubation, while uptake of polymer-modified AuNPs was observed only after 2 hours. In addition, the cellular uptake of AuNPs was reduced over time. This might have been due to cell division or due to AuNP expulsion from the cells over time, as has been observed previously.[36] We found greater uptake of PVP-modified AuNPs than mPEG-modified AuNPs. In contrast to PVP-modified AuNPs, the cellular uptake of mPEG-modified AuNPs was observed only after 24 hours of incubation. This is supported by the work of Nativo et al, who reported the absence of uptake of PEG-modified AuNPs by HeLa cells, even after prolonged incubation times or increased NP concentrations.[27] Furthermore, Hu et al demonstrated that PEG coating resulted in reduction in cellular uptake by a third compared to another polymer coating (poly[*N*-vinylcaprolactam]), which promoted the cellular uptake of NPs.[28,37] While polymer coating for enhanced retention of AuNPs may be desirable for imaging diagnostics, targeted delivery to specific sites/cells may be achieved by surface modification using mixed PEG–peptide to enable receptor-mediated endocytosis and enhance cellular internalisation.[38] The use of charged polymers containing aromatic sulfonate has also shown preferential endocytosis by ECs, due to their affinity for caveolae structures.[39]

We demonstrated that BAEC proliferation was inhibited after incubation with both unmodified AuNPs and polymer-modified AuNPs, as has been previously demonstrated in human dermal microvascular ECs.[33] In our present study, we showed that AuPVP and AumPEG had similar effects on BAEC proliferation and viability. We assessed apoptosis, also known as programmed cell death, using flow-cytometry analysis based on annexin V–FITC and PI-PE double staining, and found that AuNPs exerted significant effects in a time-dependent manner and were influenced by surface modification. Similarly, Selim and Hendi found that AuNPs induced apoptosis in MCF7 human breast cells via activation of the p53, Bax/Bcl2, and caspase pathways.[40] However, they found that significant cytotoxicity was dose-dependent, whereby at 200 μg/mL viability was 70% after 24 hours. The latter dose used was threefold higher than the one used in our study (2.9 μg/mL). Here, we showed that modified AuNPs and their stabilizers, PVP and mPEG, induced a significant increase in apoptosis. We also observed that mPEG and PVP alone significantly increased necrotic cells. The influence of AuNPs on cell death and apoptosis has been documented previously,[9,12] including PEG-modified AuNPs,[41] whereby their accumulation in tissues after in vivo administration has also been shown to alter biochemical indices of liver and kidney damage[41] and upregulates markers of acute inflammation.[42] PVP-modified AuNPs have also been demonstrated to inhibit MMP activity without any cytotoxic effects. The inhibitory effect is attributed to binding of the negatively charged surface PVP coating to Zn^{2+} moieties within MMPs.[43]

MAPK (ERK1/2) is necessary for induction of various cell functions, including proliferation, and its activated form (phospho-ERK1/2) is known to accumulate significantly in the nucleus.[44] In addition, previous studies have demonstrated the importance of ERK2 phosphorylation over ERK1 phosphorylation in cell proliferation and survival.[45] Our Western

International Journal of Nanomedicine downloaded from https://www.dovepress.com/ by 149.170.165.59 on 29-Mar-2018
For personal use only.

blot analysis showed that ERK1/2 expression was reduced in all culture conditions when compared to incubation in ACh alone. Suppression of ERK1/2 phosphorylation by AuNPs has recently been documented in human umbilical vein ECs.[13] This is also supported by our finding that both modified and unmodified AuNPs inhibited cell proliferation of BAECs. As inhibitors of the ERK1/2 pathway are emerging in clinical trials as anticancer agents,[44] our modified/unmodified AuNPs may have potential use as anticancer agents. Indeed, the antiangiogenic effects of AuNPs have recently been shown.[13]

Although unmodified AuNPs were not detectable inside ECs from the TEM images analyzed, we found evidence of their uptake using ICP-MS. A few AuNPs were detected after modification with mPEG and PVP, while an increase in concentration of mPEG-modified AuNPs led to increased vascular uptake. AuNPs were located in the cytoplasm of ECs, but none was located in the nucleus of cells, elastic lamina, or smooth-muscle cell layer. Reduced uptake of PEGylated NPs has been demonstrated previously and shown to reduce hydrophilicity, phagocytosis, and accumulation in off-target organs.[46] Reduced NP uptake may also be due to the dynamics of uptake via endocytosis/exocytosis.[9,36,47]

Aortic vessels were incubated in AuNPs at 1.68×10^{11} NPs/mL (equivalent to 2.9 μg/mL), over a 30-minute acute-exposure period. This dosage was also utilized in our cell-culture experiments. Our exposure time and NP concentration are commonly used in preclinical and clinical studies. Stern et al utilized gold-core NPs with a silica shell, infused at approximately 2.77×10^{11} NPs/mL, to ablate prostate tumors thermally.[1] In preclinical studies, AuNPs have been identified within 30 minutes of intravenous administration into mice, in the dermal papilla and root sheaths of hair follicles.[48] Intravenous injection of 13 nm PEGylated AuNPs (at 1.76×10^{11} NPs/mL) led to their accumulation in tissues within 30 minutes and induced acute inflammation and apoptosis.[42] We observed that unmodified AuNPs had no overall effect on the endothelium-dependent (ACh) relaxation of the vessels; however, they significantly attenuated responses to the endothelium-independent agonist SNP. SNP has been used clinically as an antihypertensive agent, as it acts by releasing NO, leading to dilation of small vessels. AuNPs may interact directly with the SNP drug, as has been demonstrated previously in mesenteric vessels after incubation in quantum dots.[49] Such interaction has also been suggested for a number of other agonists after pulmonary NP exposure,[50] thus confirming the additional need for surface modification of AuNPs before use.

Vessel incubation in PVP-modified AuNPs had no significant effect on ACh dilator responses; however, incubation in PVP alone (at the minimum concentration required to prevent NP aggregation) caused a significant reduction in ACh responses. In comparison, vessel incubation in PVP-modified AuNPs induced a significant reduction in SNP responses. When vessels were incubated in PVP alone, no significant effect on SNP responses was noted. This suggests that it is the AuNPs themselves that may be interfering with the action of SNP. AuNPs and PVP-modified AuNPs may compete for the NO released by the NO donors, thus impairing the vasodilator response, as has been recently demonstrated using ruthenium complex as an NO donor. When complexed with AuNPs, NO release was reduced.[51] The PVP-polymer monolayer may have been insufficient to coat the AuNPs fully, and hence allowed their interaction with SNP. AuNPs have previously been demonstrated to show intrinsic catalytic activity,[52] which can vary depending on their surface charge and the type of surface modification.[53] Using electrospin-resonance spectroscopy, He et al investigated the catalytic activity of AuNPs and demonstrated that both PVP- and tannic acid-modified 10–100 nm AuNPs rapidly catalyzed the decomposition of hydrogen peroxide, generating hydroxyl radicals at low pH and oxygen at higher pH. This has important implications in relation to AuNP uptake into the acidic environment of endosomal structures within cells. The AuNPs were also able to scavenge reactive oxygen species, catalyzing the decomposition of superoxide anions.[52] mPEG-modified AuNPs (at 2.9 μg/mL) had no overall influence on endothelium-dependent responses. When exposed to a higher 5.8 μg/mL concentration of mPEG-modified AuNPs, dilatory responses were significantly reduced ($P<0.001$). Indeed, uptake of mPEG-modified AuNPs by ECs has also been shown to be concentration-dependent by others, whereby high NP concentration may result in passive transport into vessels.[54]

In order to elucidate mechanisms leading to attenuated vasodilation by AuNPs, we conducted cellular studies to examine their influence on the ERK1/2-signaling pathway. This pathway plays an important role in stimulating the production of NO by activation of endothelial NO synthase, and has been implicated in vasodilator responses associated with retinal arterioles.[55] When BAECs were stimulated with ACh, ERK1/2 phosphorylation was maximal at 10 μM ACh concentration, in accordance with maximal aortic vasodilation, ex vivo. When BAECs were stimulated with ACh in the presence of modified and unmodified AuNPs, a reduction in ERK2 phosphorylation was observed for PVP and

International Journal of Nanomedicine downloaded from https://www.dovepress.com/ by 149.170.165.59 on 29-Mar-2018
For personal use only.

mPEG-modified AuNPs. Vessel incubation in PVP alone led to a significant reduction in ACh-induced dilation. The reason for this is not clear. The surface chemistry of the polymers, however, is known to influence cell interaction and morphology.[56,57] PVP-surface groups could bind to ACh receptors, acting as an antagonist.[58] This is supported by the rightward shift in the ACh dose–response curve, observed in our study after PVP incubation.

Conclusion

We showed that AuNP uptake by cells was dependent on surface modification and incubation time. Incubation in polymers alone also affected cellular and vasodilator functions. We showed that exposure of isolated aortic vessels to AuNPs at a dosage similar to that utilized in clinical trials[1] affected vasodilator function, but was dependent on surface modification. PVP surface-modified gold NPs inhibited EC viability, proliferation, and ERK1/2 phosphorylation, and reduced the magnitude of endothelial-independent dilator responses in aortic vessels. In contrast, mPEG-modified AuNPs showed lower cytostatic effects and were less detrimental to vasodilator function than PVP-modified AuNPs, indicating greater potential as agents for diagnostic imaging and therapy.

Acknowledgments

The authors thank Dave Maskew and Glenn Ferris, Manchester Metropolitan University, for technical support, Dr Carolyn Jones (Maternal and Fetal Health Research Group, University of Manchester), Dr Aleksander Mironov (EM Facility, Faculty of Life Sciences, University of Manchester) for sample preparation and electron microscopy, and the Wellcome Trust for equipment-grant support to the EM Facility, University of Manchester, Manchester, UK. This work was partly funded by the EPSRC-funded Bridging the Gaps: Nano-Info-Bio project (grant EP/H000291/1).

Disclosure

The authors report no conflicts of interest in this work.

References

1. Stern JM, Solomonov VV, Sazykina E, Schwartz JA, Gad SC, Goodrich GP. Initial evaluation of the safety of nanoshell-directed photothermal therapy in the treatment of prostate disease. *Int J Toxicol*. 2016;35(1):38–46.
2. Dreaden EC, Alkilany AM, Huang X, Murphy CJ, El-Sayed MA. The golden age: gold nanoparticles for biomedicine. *Chem Soc Rev*. 2012;41(7):2740–2779.
3. Nanospectra Biosciences. Pilot study of AuroLase therapy in refractory and/or recurrent tumors of the head and neck. Available from: https://clinicaltrials.gov/ct2/show/NCT00848042. NLM identifier: NCT00848042. Accessed March 16, 2017.
4. Cui W, Li J, Zhang Y, Rong H, Lu W, Jiang L. Effects of aggregation and the surface properties of gold nanoparticles on cytotoxicity and cell growth. *Nanomedicine*. 2012;8(1):46–53.
5. Alkilany AM, Yaseen AI, Kailani MH. Synthesis of monodispersed gold nanoparticles with exceptional colloidal stability with grafted polyethylene glycol-g-polyvinyl alcohol. *J Nanomater*. 2015;2015:712359.
6. Cytimmune. Aurimune: a nanomedicine platform. Available from: http://www.cytimmune.com/user. Accessed March 16, 2017.
7. Libutti SK, Paciotti GF, Byrnes AA, et al. Phase I and pharmacokinetic studies of CYT-6091, a novel PEGylated colloidal gold-rhTNF nanomedicine. *Clin Cancer Res*. 2010;16(24):6139–6149.
8. Uchiyama MK, Deda DK, Rodrigues SF, et al. In vivo and in vitro toxicity and anti-inflammatory properties of gold nanoparticle bioconjugates to the vascular system. *Toxicol Sci*. 2014;142(2):497–507.
9. Tsai SW, Liaw JW, Kao YC, et al. Internalized gold nanoparticles do not affect the osteogenesis and apoptosis of MG63 osteoblast-like cells: a quantitative, in vitro study. *PLoS One*. 2013;8(10):e76545.
10. Coulter JA, Jain S, Butterworth KT, et al. Cell type-dependent uptake, localization, and cytotoxicity of 1.9 nm gold nanoparticles. *Int J Nanomedicine*. 2012;7:2673–2685.
11. Tarasova NK, Gallud A, Ytterberg AJ, et al. Cytotoxic and proinflammatory effects of metal-based nanoparticles on THP-1 monocytes characterized by combined proteomics approaches. *J Proteome Res*. 2017;16(2):689–697.
12. Leite PE, Pereira MR, Santos CA, Campos AP, Esteves TM, Granjeiro JM. Gold nanoparticles do not induce myotube cytotoxicity but increase the susceptibility to cell death. *Toxicol In Vitro*. 2015;29(5):819–827.
13. Roh YJ, Rho CR, Cho WK, Kang S. The antiangiogenic effects of gold nanoparticles on experimental choroidal neovascularization in mice. *Invest Ophthalmol Vis Sci*. 2016;57(15):6561–6567.
14. Shrivastava R, Kushwaha P, Bhutia YC, Flora S. Oxidative stress following exposure to silver and gold nanoparticles in mice. *Toxicol Ind Health*. 2016;32(8):1391–1404.
15. Soenen SJ, Manshian BB, Abdelmonem AM, et al. The cellular interactions of PEGylated gold nanoparticles: effects of PEGylation on cellular uptake and cytotoxicity. *Part Part Syst Charact*. 2014;31(7):794–800.
16. Wan J, Wang JH, Liu T, Xie Z, Yu XF, Li W. Surface chemistry but not aspect ratio mediates the biological toxicity of gold nanorods in vitro and in vivo. *Sci Rep*. 2015;5:11398.
17. Alkilany AM, Shatanawi A, Kurtz T, Caldwell RB, Caldwell RW. Toxicity and cellular uptake of gold nanorods in vascular endothelium and smooth muscles of isolated rat blood vessel: importance of surface modification. *Small*. 2012;8(8):1270–1278.
18. Liu X, Xu Y, Wu Z, Chen H. Poly(N-vinylpyrrolidone)-modified surfaces for biomedical applications. *Macromol Biosci*. 2013;13(2):147–154.
19. Zhi X, Fang H, Bao C, et al. The immunotoxicity of graphene oxides and the effect of PVP-coating. *Biomaterials*. 2013;34(21):5254–5261.
20. Farooq A, Whitehead D, Azzawi M. Attenuation of endothelial-dependent vasodilator responses, induced by dye-encapsulated silica nanoparticles, in aortic vessels. *Nanomedicine (Lond)*. 2014;9(3):413–425.
21. Turkevich J, Stevenson PC, Hillier J. A study of the nucleation and growth processes in the synthesis of colloidal gold. *Discuss Faraday Soc*. 1951;11:55–75.
22. Sattar A, Rooney P, Kumar S, et al. Application of angiogenic oligosaccharides of hyaluronan increases blood vessel numbers in rat skin. *J Invest Dermatol*. 1994;103(4):576–579.
23. Boras E, Slevin M, Alexander MY, et al. Monomeric C-reactive protein and Notch-3 cooperatively increase angiogenesis through PI3K signalling pathway. *Cytokine*. 2014;69(2):165–179.
24. Gangwar RK, Dhumale VA, Kumari D, et al. Conjugation of curcumin with PVP capped gold nanoparticles for improving bioavailability. *Mater Sci Eng C Mater Biol Appl*. 2012;32(8):2659–2663.
25. Manson J, Kumar D, Meenan BJ, Dixon D. Polyethylene glycol functionalized gold nanoparticles: the influence of capping density on stability in various media. *Gold Bull*. 2011;44(2):99–105.
26. Frost M, Dempsey M, Whitehead D. The response of citrate functionalised gold and silver nanoparticles to the addition of heavy metal ions. *Colloids Surf A Physicochem Eng Asp*. 2017;518:15–24.

International Journal of Nanomedicine downloaded from https://www.dovepress.com/ by 149.170.165.59 on 29-Mar-2018
For personal use only.

27. Nativo P, Prior IA, Brust M. Uptake and intracellular fate of surface-modified gold nanoparticles. *ACS Nano*. 2008;2(8):1639–1644.
28. Araki J, Mishima S. Steric stabilization of charge free cellulose nanowhiskers by grafting of polyethylene glycol. *Molecules*. 2015;20(1):169–184.
29. Huynh KA, Chen KL. Aggregation kinetics of citrate and polyvinylpyrrolidone coated silver nanoparticles in monovalent and divalent electrolyte solutions. *Environ Sci Technol*. 2011;45(13):5564–5571.
30. Afshinnia K, Sikder M, Cai B, Baalousha M. Effect of nanomaterial and media physicochemical properties on Ag NM aggregation kinetics. *J Colloid Interface Sci*. 2017;487:192–200.
31. Xiong Y, Washio I, Chen J, Cai Z, Li Y, Xia Y. Poly(vinyl pyrrolidone): a dual functional reductant and stabilizer for the facile synthesis of noble metal nanoplates in aqueous solutions. *Langmuir*. 2006;22(20):8563–8570.
32. Wang J, Wang L, Sun Y, et al. Surface plasmon resonance biosensor based on Au nanoparticle in titania sol-gel membrane. *Colloids Surf B Biointerfaces*. 2010;75(2):520–525.
33. Freese C, Gibson MI, Klok HA, Unger RE, Kirkpatrick CJ. Size- and coating-dependent uptake of polymer-coated gold nanoparticles in primary human dermal microvascular endothelial cells. *Biomacromolecules*. 2012;13(5):1533–1543.
34. Rahman WN, Bishara N, Ackerly T, et al. Enhancement of radiation effects by gold nanoparticles for superficial radiation therapy. *Nanomedicine*. 2009;5(2):136–142.
35. Chithrani BD, Ghazani AA, Chan WC. Determining the size and shape dependence of gold nanoparticle uptake into mammalian cells. *Nano Lett*. 2006;6(4):662–668.
36. Mironava T, Hadjiargyrou M, Simon M, Jurukovski V, Rafailovich MH. Gold nanoparticles cellular toxicity and recovery: effect of size, concentration and exposure time. *Nanotoxicology*. 2010;4(1):120–137.
37. Hu L, Mao ZW, Gao CY. Colloidal particles for cellular uptake and delivery. *J Mater Chem*. 2009;19(20):3108–3115.
38. Liu Y, Shipton MK, Ryan J, Kaufman ED, Franzen S, Feldheim DL. Synthesis, stability, and cellular internalization of gold nanoparticles containing mixed peptide-poly(ethylene glycol) monolayers. *Anal Chem*. 2007;79(6):2221–2229.
39. Voigt J, Christensen J, Shastri VP. Differential uptake of nanoparticles by endothelial cells through polyelectrolytes with affinity for caveolae. *Proc Natl Acad Sci U S A*. 2014;111(8):2942–2947.
40. Selim ME, Hendi AA. Gold nanoparticles induce apoptosis in MCF-7 human breast cancer cells. *Asian Pac J Cancer Prev*. 2012;13(4):1617–1620.
41. Zhang XD, Wu D, Shen X, et al. Size-dependent in vivo toxicity of PEG-coated gold nanoparticles. *Int J Nanomedicine*. 2011;6:2071–2081.
42. Cho WS, Cho M, Jeong J, et al. Acute toxicity and pharmacokinetics of 13 nm-sized PEG-coated gold nanoparticles. *Toxicol Appl Pharmacol*. 2009;236(1):16–24.
43. Hashimoto M, Sasaki JI, Yamaguchi S, et al. Gold nanoparticles inhibit matrix metalloproteases without cytotoxicity. *J Dent Res*. 2015;94(8):1085–1091.
44. Roux PP, Blenis J. ERK and p38 MAPK-activated protein kinases: a family of protein kinases with diverse biological functions. *Microbiol Mol Biol Rev*. 2004;68(2):320–344.
45. D'Souza WN, Chang CF, Fischer AM, Li M, Hedrick SM. The Erk2 MAPK regulates CD8 T cell proliferation and survival. *J Immunol*. 2004;181(11):7617–7629.
46. Arnida, Janát-Amsbury MM, Ray A, Peterson CM, Ghandehari H. Geometry and surface characteristics of gold nanoparticles influence their biodistribution and uptake by macrophages. *Eur J Pharm Biopharm*. 2011;77(3):417–423.
47. Oh N, Park JH. Endocytosis and exocytosis of nanoparticles in mammalian cells. *Int J Nanomedicine*. 2014;9:51–63.
48. Kempson IM, Chien CC, Chung CY, et al. Fate of intravenously administered gold nanoparticles in hair follicles: follicular delivery, pharmacokinetic interpretation, and excretion. *Adv Healthc Mater*. 2012;1(6):736–741.
49. Shukur A, Rizvi SB, Whitehead D, Seifalian A, Azzawi M. Altered sensitivity to nitric oxide donors, induced by intravascular infusion of quantum dots, in murine mesenteric arteries. *Nanomedicine*. 2013;9(4):532–539.
50. Nurkiewicz TR, Porter DW, Hubbs AF, et al. Pulmonary nanoparticle exposure disrupts systemic microvascular nitric oxide signaling. *Toxicol Sci*. 2009;110(1):191–203.
51. Silva BR, Lunardi CN, Araki K, Biazzotto JC, Da Silva RS, Bendhack LM. Gold nanoparticle modifies nitric oxide release and vasodilation in rat aorta. *J Chem Biol*. 2014;7(2):57–65.
52. He W, Zhou YT, Wamer WG, et al. Intrinsic catalytic activity of Au nanoparticles with respect to hydrogen peroxide decomposition and superoxide scavenging. *Biomaterials*. 2013;34(3):765–773.
53. Wang S, Chen W, Liu AL, Hong L, Deng HH, Lin XH. Comparison of the peroxidase-like activity of unmodified, amino-modified, and citrate-capped gold nanoparticles. *Chemphyschem*. 2012;13(5):1199–1204.
54. Treuel L, Jiang X, Nienhaus GU. New views on cellular uptake and trafficking of manufactured nanoparticles. *J R Soc Interface*. 2013;10(82):20120939.
55. Yuan Z, Hein TW, Rosa RH Jr, Kuo L. Sildenafil (Viagra) evokes retinal arteriolar dilation: dual pathways via NOS activation and phosphodiesterase inhibition. *Invest Ophthalmol Vis Sci*. 2008;49(2):720–725.
56. Ionov M, Tukfatullina I, Salakhutdinov B, Baram N, Bryszewska M, Aripov T. The interaction of PVP complexes of gossypol and its derivatives with an artificial membrane lipid matrix. *Cell Mol Biol Lett*. 2010;15(1):98–117.
57. Saltzman WM. Cell interactions with polymers. In Lanza RP, Langer R, Vacanti J, editors. *Textbook of Tissue Engineering*. 2nd ed. New York: Academic Press; 2000:221–235.
58. Jiang Y, Yan YB, Zhou HM. Polyvinylpyrrolidone 40 assists the refolding of bovine carbonic anhydrase B by accelerating the refolding of the first molten globule intermediate. *J Biol Chem*. 2006;281(14):9058–9065.

International Journal of Nanomedicine downloaded from https://www.dovepress.com/ by 149.170.165.59 on 29-Mar-2018
For personal use only.

Supplementary materials

Surface-enhanced Raman spectroscopy

For sample preparation, 1 mL gold nanoparticle (AuNP) solution was drop-coated on the glass slide and left to dry in the oven overnight, then Raman spectra were recorded the following day. The spectra were obtained with a microscopic confocal Raman spectrometry, operated with an argon laser (514 nm). The laser intensity was 50 mW. Surface-enhanced Raman spectroscopy analysis showed the vibration frequency of the functional groups on AuNPs, identified by the peaks of the groups present within Au polyvinylpyrrolidone (AuPVP) and Au mercapto polyethylene glycol (AumPEG) and the types of bonds present in the chemical compounds. The spectra showed that the AuNPs were functionalized, as the wavelength of the functional groups were identified and demonstrated to be present. The results indicated the shifting of the C=O peak from 1,521 cm^{-1} in the citrate-stabilized AuNPs to 1,649 cm^{-1}, which was attributed to the hydrogen bonding between the mPEG and citrate ligands. The peak shifted to 1,609 cm^{-1} after the surface had been stabilized with PVP (Figure S1).

Flow cytometry

Cell viability

Flow-cytometry analysis was performed after 30 minutes and 2–24 and 48 hours of bovine aortic endothelial cell (BAEC) treatment with stabilizers and unmodified and modified AuNPs, followed by staining with propidium iodide (PI)–phycoerythrin (PE). Representative dot blots are shown in Figure S2A.

Cell apoptosis and necrosis

Flow-cytometry analysis was performed after 2 and 24 hours of BAEC treatment with stabilizers and unmodified and modified AuNPs, followed by double staining with annexin V–fluorescein isothiocyanate/PI-PE (Figure S2B).

Vasodilator responses to mPEG-modified AuNPs

In a separate set of experiments, the influence of a double concentration of mPEG-modified AuNPs (at 5.8 µg/mL) on vasodilator function was assessed. A significant reduction in acetylcholine-induced dilator function was observed (Figure S3).

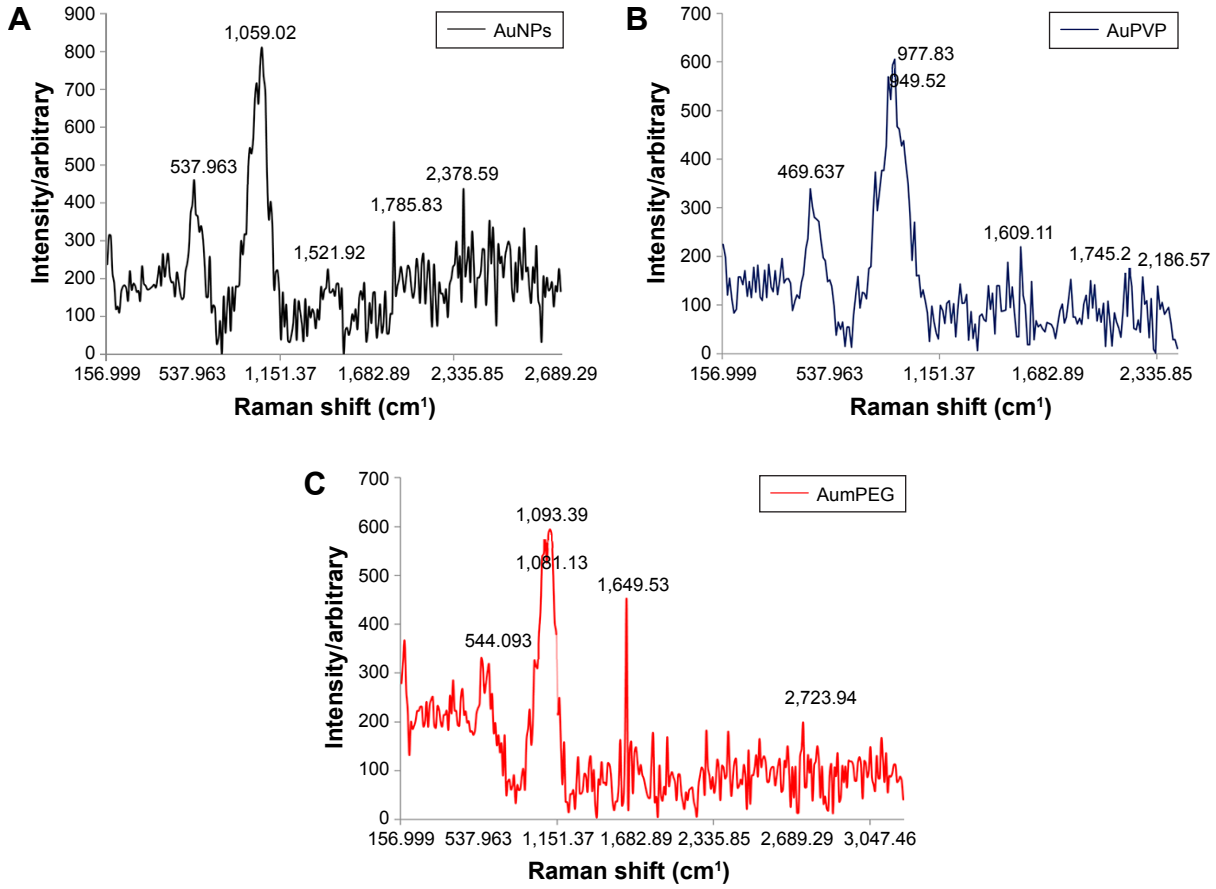

Figure S1 Surface-enhanced Raman spectroscopy analysis for unmodified and modified AuNPs.
Note: Unmodified AuNPs (**A**), mPEG-modified AuNPs (**B**), and PVP-modified AuNPs (**C**).
Abbreviations: AuNPs, gold nanoparticles; mPEG, mercapto polyethylene glycol; PVP, polyvinylpyrrolidone.

International Journal of Nanomedicine downloaded from https://www.dovepress.com/ by 149.170.165.59 on 29-Mar-2018
For personal use only.

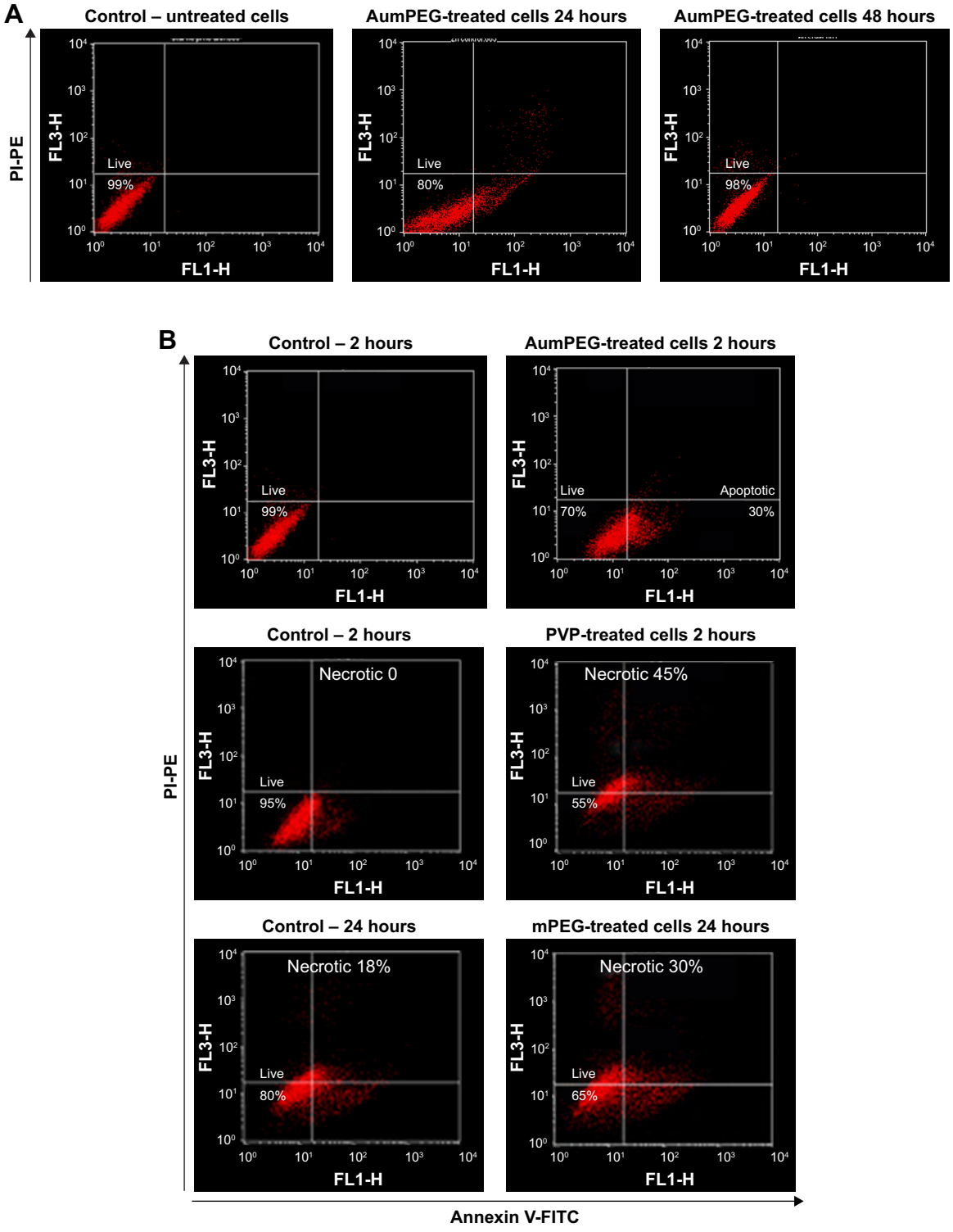

Figure S2 Flow-cytometry analysis of cell viability, apoptosis, and necrosis after AuNP exposure.

Notes: (**A**) Cell viability of BAECs in untreated cells and in cells treated with AumPEG after 24 and 48 hours. Numbers within dot plots represent the percentage of live cells (lower left, PI^-). (**B**) Induction of apoptosis by AumPEG after 2 hours' exposure, showing induction of necrosis by stabilizers after 2 and 24 hours' exposure in comparison with untreated cells.

Abbreviations: AuNP, gold nanoparticle; BAECs, bovine aortic endothelial cells; mPEG, mercapto polyethylene glycol; PI, propidium iodide; PE, phycoerythrin; PVP, polyvinylpyrrolidone.

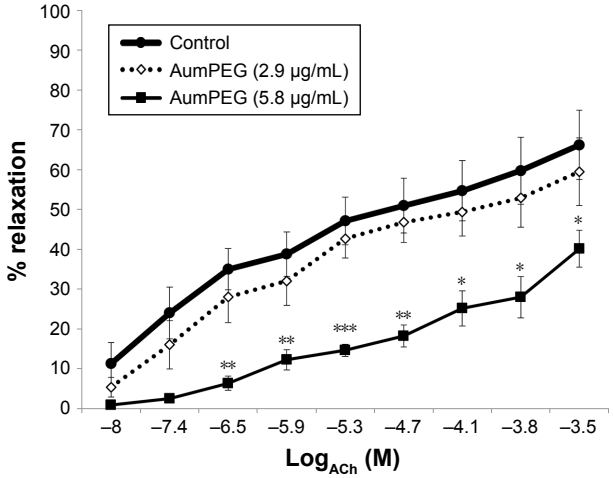

Figure S3 Influence of mPEG-modified AuNPs on endothelial-dependent dilator responses of aortic vessels.
Notes: *$P<0.05$; **$P<0.01$; ***$P<0.001$. Endothelial-dependent (ACh) dilator responses of preconstricted aortic vessels after 30 minutes' exposure of high-concentration mPEG-modified AuNPs (5.8 µg/mL) ex vivo. Error bars are SEM.
Abbreviations: AuNPs, gold nanoparticles; mPEG, mercapto polyethylene glycol; PVP, polyvinylpyrrolidone.

International Journal of Nanomedicine downloaded from https://www.dovepress.com/ by 149.170.165.59 on 29-Mar-2018
For personal use only.

International Journal of Nanomedicine
Dovepress
Publish your work in this journal
The International Journal of Nanomedicine is an international, peer-reviewed journal focusing on the application of nanotechnology in diagnostics, therapeutics, and drug delivery systems throughout the biomedical field. This journal is indexed on PubMed Central, MedLine, CAS, SciSearch®, Current Contents®/Clinical Medicine, Journal Citation Reports/Science Edition, EMBase, Scopus and the Elsevier Bibliographic databases. The manuscript management system is completely online and includes a very quick and fair peer-review system, which is all easy to use. Visit http://www.dovepress.com/testimonials.php to read real quotes from published authors.
Submit your manuscript here: http://www.dovepress.com/international-journal-of-nanomedicine-journal